scientific reports

Check for updates

OPEN

Autoantibody spark response predicts treatment outcome in patients receiving chemoradiation followed by durvalumab therapy

Takeru Mori[1], Mio Kitagawa[2], Tomokazu Hasegawa[2], Masanori Someya[2], Takaaki Tsuchiya[2], Toshio Gocho[2], Tomoko Honjo[1], Mirei Date[1], Mariko Morii[1], Ai Miyamoto[1] & Junichiro Futami[1]✉

The PACIFIC regimen, comprising chemoradiotherapy (CRT) followed by maintenance with the immune checkpoint inhibitor (ICI) durvalumab, has become the standard of care for patients with unresectable non-small cell lung cancer (NSCLC). Although ICI is used to prevent recurrence by targeting residual microtumors, biomarkers capable of monitoring immune activity during this phase remain lacking. Here, we evaluated whether temporal changes in serum autoantibody levels can predict treatment efficacy. This retrospective study included 20 patients with unresectable stage II or III NSCLC who received the PACIFIC regimen. Serum autoantibodies against 130 antigens were quantified before CRT, after CRT, and two weeks after the first ICI dose. The primary outcome was progression-free survival (PFS), and its association with autoantibody dynamics was examined. We observed an immediate and strong autoantibody response (spark response [SR]) after ICI initiation in patients with favorable treatment outcomes. Patients with SR and programmed death ligand 1 (PD-L1) expression ≥ 50% showed better PFS (two-year PFS; 72.9% vs. 18.2%, $p = 0.0021$). These findings suggest that serial monitoring of serum autoantibodies can provide a noninvasive approach to assess immune activity and predict treatment outcomes in patients receiving CRT or ICI therapy.

Keywords Autoantibodies, PACIFIC regimen, ICIs, Immune monitoring

Abbreviations

CI	Confidence intervals
CR	Complete response
CRT	Chemoradiotherapy
CTAs	Cancer-testis antigens
HSR	Hyper-spark response
ICI	Immune checkpoint inhibitor
MFI	Mean fluorescence intensity
MUSCAT	Multiple S-cationized antigen immobilized beads array assay
NSCLC	Non-small cell lung cancer
PBMCs	Peripheral blood mononuclear cells
PD	Progressive disease
PD-L1	Programmed death ligand 1
PFS	Progression-free survival
SR	Spark response
TAAs	Tumor-associated antigens
TLS	Tertiary lymphoid structure
TPS	Tumor proportion score
WR	Weak response

[1]Graduate School of Interdisciplinary Science and Engineering in Health Systems, Okayama University, 3-1-1 Tsushima-Naka, Okayama 700-8530, Japan. [2]Department of Radiology, Sapporo Medical University School of Medicine, Sapporo, Japan. ✉email: futamij@okayama-u.ac.jp

The PACIFIC regimen, comprising concurrent chemoradiotherapy (CRT) followed by 12 months of durvalumab for immune consolidation, is the standard treatment for unresectable stage III non-small cell lung cancer (NSCLC)[1–3]. This regimen has significantly improved the five-year overall survival and progression-free survival (PFS) compared with CRT alone[3]. Durvalumab is an immune checkpoint inhibitor (ICI) targeting programmed death ligand 1 (PD-L1) and helps prevent disease recurrence by enhancing antitumor immune responses[4,5]. The tumor proportion score (TPS), which measures PD-L1 expression in pre-CRT biopsy samples, is a well-established predictive biomarker for ICI responsiveness[6,7]. However, after CRT, tumors often shrink to clinically undetectable levels, making repeat biopsies unfeasible. Therefore, noninvasive biomarkers that can capture the activation of the cancer-immunity cycle and support clinical decision-making during ICI treatment are necessary.

Although serum autoantibody levels remain low in healthy volunteers because of immune tolerance[8], chronic autoimmunity and antitumor responses can stimulate their production[9]. Tumor-associated antigens (TAAs)[10,11] and cancer testis antigens (CTAs)[12], expressed by tumor cells stimulate autoantibody production and activation of the cancer-immunity cycle[13]. Therefore, anti-TAA/CTA autoantibodies are promising biomarkers for predicting ICI-induced antitumor responses[14,15]. Notably, the levels of autoantibodies commonly associated with autoimmunity are elevated in patients with cancer, underscoring the close relationship between autoimmune and antitumor immune responses[16].

However, clinical analysis of autoantibodies faces several challenges. Autoantibody profiles vary significantly among individuals, necessitating the use of semicomprehensive arrays for accurate assessment[17]. Additionally, many TAAs/CTAs are prone to aggregation and exhibit unstable properties, thereby requiring high-purity autoantigen preparation and repeatable and precise assays[18,19]. The multiple *S*-cationized antigen-immobilized bead array assay (MUSCAT assay) addresses these challenges by combining protein solubilization of denatured antigens with the Luminex system, enabling robust and reproducible detection of serum autoantibodies[20,21].

In our previous preliminary study, serum autoantibody levels analyzed using the MUSCAT assay were confirmed to be higher in patients with prostate cancer than in healthy volunteers[20]. Additionally, increased levels of several autoantibodies have been observed before tumor regression in patients with a good prognosis after receiving cancer gene therapy. Thus, autoantibody monitoring may serve as liquid biomarkers for monitoring antitumor immune responses.

Accordingly, we hypothesized that the temporal monitoring of serum autoantibodies could capture immune activation in patients with NSCLC receiving the PACIFIC regimen. Using the MUSCAT assay, we assessed autoantibody dynamics throughout the treatment period, demonstrating its potential as a noninvasive biomarker to support clinical decisions.

Methods

Patients and clinical samples

This retrospective cohort study included 20 patients with pathologically confirmed unresectable stage II or III NSCLC who underwent concurrent CRT followed by ICI therapy with durvalumab at Sapporo Medical University Hospital between July 2020 and November 2023[22]. Among the 32 patients who received definitive CRT, those who achieved a complete response (CR) or partial response to CRT and subsequently received at least one cycle of ICI as maintenance therapy within 2–4 weeks after CRT completion were selected. All enrolled patients were determined to have unresectable tumors based on their clinical staging or previous treatment history. The primary endpoint of the study was PFS, which was defined as the time from the date of CRT initiation to disease recurrence. Patients who remained recurrence-free were classified as having CR, and those who developed local or distant recurrence were classified as having progressive disease (PD). All patients underwent fluorodeoxyglucose positron emission tomography and contrast-enhanced chest computed tomography for the initial staging. The treatment consisted of radiotherapy delivered in 30 fractions (totaling 60 Gy) in combination with platinum-based chemotherapy. ICI consolidation therapy was initiated 2–4 weeks after CRT completion and administered every two weeks for 24 cycles. ICI was discontinued upon the development of grade ≥ 2 radiation pneumonitis, immune-related adverse events, or confirmed disease progression, and patients were subsequently switched to salvage chemotherapy. The characteristics of the 20 patients with NSCLC are summarized in Tables 1 and 2.

Serum samples were collected on the day CRT commenced (pre-CRT), on the final day of CRT (post-CRT), and two weeks after the first dose of ICI (post-1st ICI) (Fig. 1B). These samples were stored at − 80 °C until further analysis for immune monitoring. The TPS was assessed using formalin-fixed, paraffin-embedded tumor biopsy samples obtained before CRT initiation. Tissue sections were mounted and stained with an anti-PD-L1 antibody (22C3; Dako).

Ethics declarations

This study was approved by the Institutional Review Board of Sapporo Medical University (no. 352 – 144) following the ethical guidelines of the Declaration of Helsinki. Written informed consent for the use of samples and medical records was obtained from all patients.

Autoantibody assay using the MUSCAT-assay panel

A total of 130 highly purified antigens (Table S1) were immobilized onto Bio-Plex Pro Magnetic COOH Beads (Bio-Rad), which were specifically designed for the assay panel (color codes #26, 27, 35, 36, 37, 43, 44, 45, 46, 52, 53, 54, 55, 62, 63, and 64) following the manufacturer's instructions. The antigen panel comprised 54 CTAs, 34 TAAs, 14 tumor markers, and 28 autoimmune antigens (Table S1). CTAs were selected from the cancer-testis antigen database[12] and catalogs of testis-specific proteins that are aberrantly expressed in cancer cells. TAAs were selected from a prioritized list for translational cancer vaccine research[11]. Additionally, the panel included 21

Age (years), median (range)		69 (53– 79)
Observation time (months), median (range)		25.5 (11.5–55.8)
Sex, N (%)	Male	17 (85)
	Female	3 (15)
Histology, N (%)	Adenocarcinoma	8 (40)
	Squamous cell carcinoma	11 (55)
	NSCLC NOS	1 (5)
Molecular alteration, N (%)	Wild type	17 (85)
	KRAS mutation	1 (5)
	ROS1 fusion	1 (5)
	not assessed	1 (5)
Disease stage, N (%)	IIB	4 (20)
	IIIA	7 (35)
	IIIB	6 (30)
	IIIC	3 (15)
ECOG PS, N (%)	0	15 (75)
	1	5 (25)
Smokers, N (%)	Non-smoker	1 (5)
	Smoker	19 (95)
PD-L1 (TPS), N (%)	≥ 50%	6 (30)
	1–49%	9 (45)
	< 1%	4 (20)
	not assessed	1 (5)
Radiotherapy, N (%)	60 Gy in 30 fractions	20 (100)
Regimen of chemotherapy, N (%)	CDDP + VNR q3w	8 (40)
	CBDCA + PTX weekly	10 (50)
	CBDCA + S-1 q3w	2 (10)
Cycles of Durvalmab, N (%)	1–5	4 (20)
	6–15	7 (35)
	completed	9 (45)
Clinical outcomes	CR (recurrence-free)	9 (45)
	PD (local recurrence or distant metastasis)	11 (55)
Radiation pneumonitis, N (%)	Grade 0–1	15 (75)
	Grade 2	5 (25)
irAE (Thyroiditis), N (%)	Grade 0	18 (90)
	Grade 1	1 (5)
	Grade 2	1 (5)

Table 1. Clinical information of the NSCLC patients ($n = 20$). *CBDCA* carboplatin, *CDDP* cisplatin, *CR* Complete response, *irAE* immune-related adverse events; *NOS* not otherwise specified, *NSCLC* non-small cell lung cancer, *PD* Progressive disease, *PTX* paclitaxel, *TPS* tumor proportion score, *VNR* vinorelbine.

autoantibody biomarkers identified using proteomic analysis of NSCLC in our laboratory[23]. Antigen preparation and assay validation were performed as previously described[20,21,24].

The bead-based assay was configured for 8–16-plex analysis with 1000 beads per antigen-immobilized bead type loaded into a 96-well microplate (Greiner Bio-One, Tokyo, Japan). Beads were blocked using Block Ace (DS Pharma Biomedical, Japan) and subsequently incubated with patient serum samples diluted 200-fold. After washing with the Bio-Plex Pro Wash Station (Bio-Rad), antigen-bound antibodies were detected using the appropriate secondary antibodies[20]. Data acquisition and analyses were conducted using the Bio-Plex 200 system (Bio-Rad), with mean fluorescence intensity (MFI) values calculated based on a minimum of 50 bead events per antigen. Samples with autoantibody titers exceeding the maximum measurement sensitivity (MFI > 25000) were re-evaluated using an 800-fold dilution, and the results were adjusted to equivalent values for 200-fold dilution.

Evaluation of ICI-induced immune responses

The immune responses triggered by ICIs were evaluated by calculating the fold change (post-first ICI/post-CRT) and difference (post-first ICI – post-CRT) in MFI values. The analysis excluded autoantibodies with a post-CRT MFI value of zero. Based on the fold change and difference in autoantibody MFI values, we categorized the immune responses into no response (NR), weak response (WR), spark response (SR), and hyper-spark response (HSR). The criteria for these categories were determined by assessing various cutoff combinations; fold changes

		CR ($n=9$)	PD ($n=11$)
Age (years), median (range)		71 (61–79)	68 (57–73)
Observation time (months), median (range)		25.2 (11.5–55.1)	27.2 (15.8–55.8)
Recurrence time (months), median (range)		Recurrence-free	11.2 (5.4–22.8)
Sex, N (%)	Male	6	11
	Female	3	0
Histology, N (%)	Adenocarcinoma	2	6
	Squamous cell carcinoma	6	5
	NSCLC NOS	1	0
Molecular alteration, N (%)	Wild type	8	9
	KRAS mutation	0	1
	ROS1 fusion	0	1
	Not assessed	1	0
Disease stage, N (%)	IIB	2	2
	IIIA	4	3
	IIIB	2	4
	IIIC	1	2
ECOG PS, N (%)	0	4	11
	1	5	0
Smokers, N (%)	Non-smoker	0	1
	Smoker	9	10
PD-L1 (TPS), N (%)	≥ 50%	5	1
	1–49%	1	8
	< 1%	2	2
	Not assessed	1	0
Regimen of chemotherapy, N (%)	CDDP + VNR q3w	2	6
	CBDCA + PTX weekly	5	5
	CBDCA + S-1 q3w	2	0
Cycles of Durvalmab, N (%)	1–5	3	1
	6–15	1	6
	Completed	5	4
Radiation pneumonitis, N (%)	Grades 0–1	9	6
	Grade 2	0	5
SR/HSR, N (%)	With	5	2
	Without	4	9
irAE (Thyroiditis), N (%)	Grade 0	8	10
	Grade 1	0	1
	Grade 2	1	0

Table 2. Comparison of clinical information by PACIFIC regimen treatment outcome (CR vs. PD). *CBDCA* carboplatin, *CDDP* cisplatin, *CR* Complete response, *irAE* immune-related adverse events; *NOS* not otherwise specified, *NSCLC* non-small cell lung cancer, *PD* Progressive disease, *PTX* paclitaxel, *TPS* tumor proportion score, *VNR* vinorelbine.

of 1.5, 2, 3, 5, 10, and 50 and difference thresholds of 500, 1000, 2000, 3000, 4000, 5000, 10,000, 15,000, and 20,000 (Figure S1). The optimal cutoff values for SR/HSR were selected by comparing the number of patients with autoantibodies meeting both conditions against clinical outcomes.

Immune cell dynamics assessed via PBMC-derived RNA-seq following ICI therapy.

To investigate whether autoantibody production was associated with B cell activation, we performed immune cell profiling using the microenvironment cell population-counter algorithm on bulk RNA-seq data derived from peripheral blood mononuclear cells (PBMCs). Among the 20 patients with NSCLC enrolled in this study, RNA-seq analysis was performed on samples from five individuals. RNA was collected both before and after ICI administration, and the fold change in estimated B cell abundance (post-first ICI / post-CRT) was calculated for each patient. This represents a re-analysis of transcriptomic data from our previous study[22].

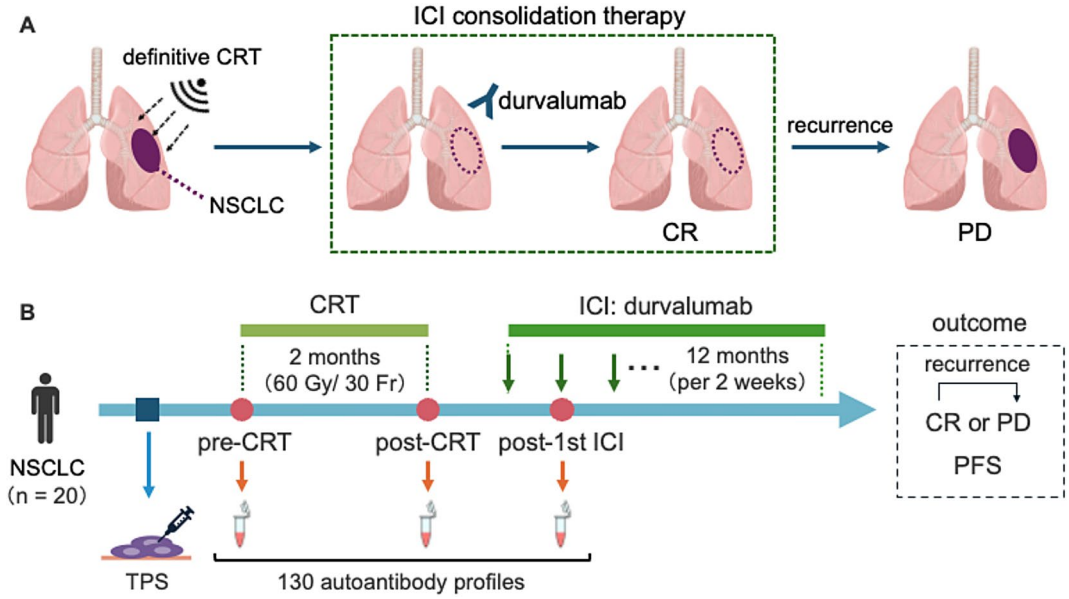

Fig. 1. Autoantibody monitoring for predicting treatment efficacy of the PACIFIC regimen. (**A**) Overview of the PACIFIC regimen of definitive CRT followed by durvalumab consolidation therapy. (**B**) Autoantibody profiles were assessed using a 130-antigen panel at three clinical time points: pre-CRT, post-CRT, and post-1st ICI. TPS were assessed before CRT initiation. The primary endpoint of the study was PFS. *CRT* chemoradiotherapy, *ICI* immune checkpoint inhibitor, *CR* recurrence-free group, *PD* non-CR group, *PFS* progression-free survival, *TPS* tumor proportion score.

Group stratification based on immune induction levels

The patients were stratified into two groups based on SR/HSR and TPS. Patients exhibiting an SR/HSR of autoantibodies or a TPS ≥ 50% were classified into Group 1 (high immune induction group), whereas the others were categorized into Group 2 (low immune induction group). To visualize the clinical events during the observation period, swimmer plots were generated for both groups. The two-year PFS was compared between both groups.

Statistical analysis

Statistical analyses were performed using R version 4.2.0. PFS was analyzed using the Kaplan–Meier method, and differences between groups were evaluated using the log-rank test. Associations between the autoantibody responses and clinical outcomes were assessed. Heatmaps were generated using the "pheatmap" package, and swimmer plots were generated using the "swimplot" package. Kaplan–Meier plots and log-rank p values were produced using the "survival" and "survminer" packages. Two-year PFS rates and their 95% confidence intervals (CIs) were calculated. All figures were generated using ggplot2 or GraphPad Prism 9.

Results

Clinical characterization of patients

Twenty patients with NSCLC (Table 1) were treated with CRT and ICIs using the PACIFIC regimen. The cutoff date for the analysis was March 2025. During analysis, the median observation time for all patients was 25.5 (11.5–55.8) months. Nine patients were recurrence-free (CR group), and 11 patients (PD group) developed local recurrence or distant metastasis at a median of 11.2 (5.4–22.8) months. Three patients died of the primary disease and eight patients survived (Table 2).

ICI consolidation therapy was completed as planned in nine patients. Treatment was terminated in five patients owing to recurrence during therapy, and five patients discontinued treatment owing to radiation pneumonitis or adverse events (Table 2).

Autoantibody monitoring

To investigate whether serum autoantibodies reflect the antitumor immune activation induced by CRT and ICI therapy (Fig. 1A), we analyzed serum samples from 20 patients with NSCLC treated with the PACIFIC regimen. Autoantibody profiles were assessed using a 130-antigen panel at pre-CRT, post-CRT, and post-first ICI (Fig. 1B). The autoantibody profiles displayed distinct individual patterns (Fig. 2A, S2A), suggesting that diverse antigens elicited antitumor immune responses across the patient cohort. Notably, a marked increase in the autoantibody levels was observed in some patients after ICI therapy (Fig. 2A, S2A). We hypothesized that favorable antitumor immune responses to the PACIFIC regimen would be associated with increased levels of serum autoantibodies and the strength of this response would be important in predicting clinical outcomes.

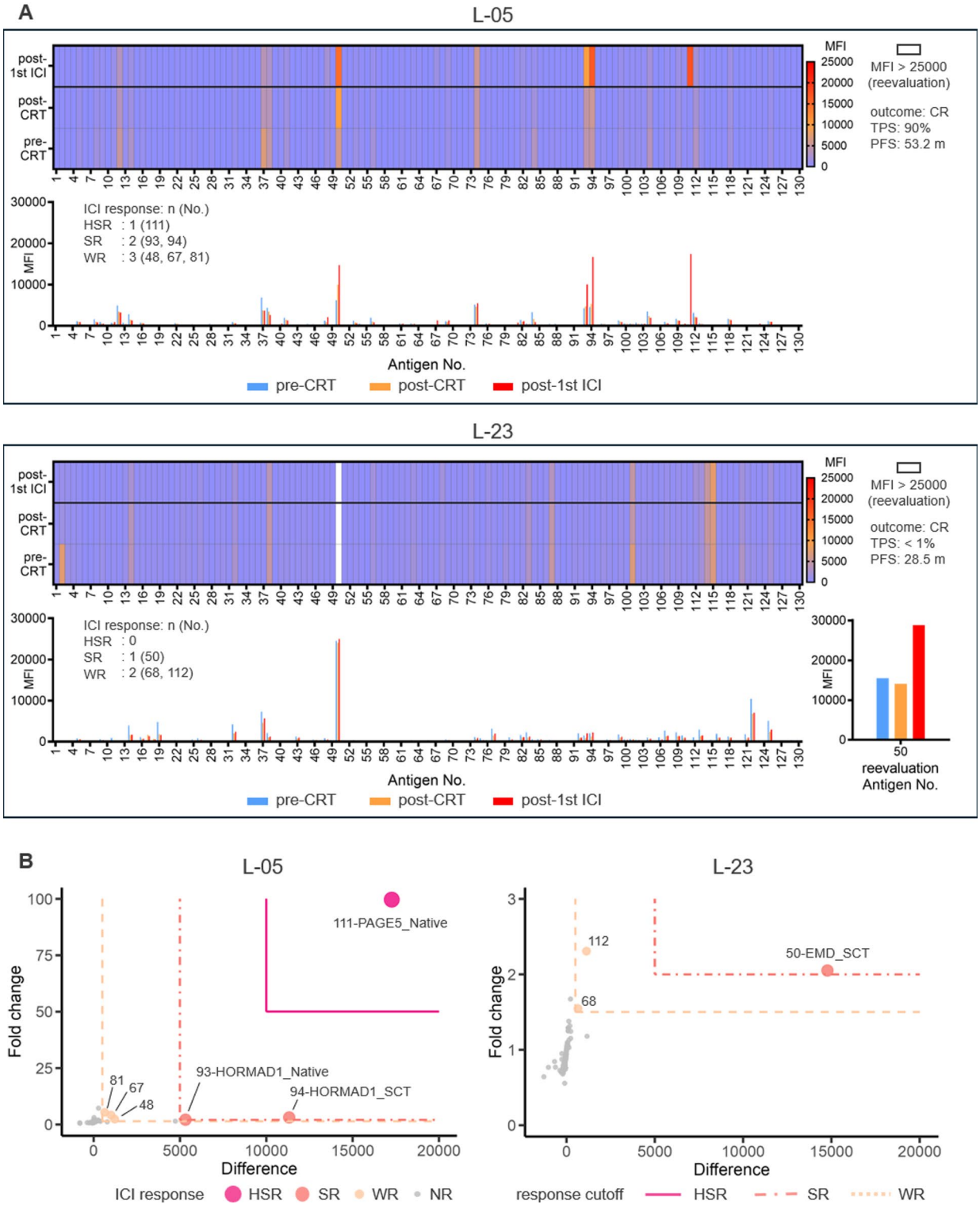

Fig. 2. Autoantibody monitoring and definition of immune response level. Two patients (L-05 and L-23, exhibiting a favorable prognosis under the PACIFIC regimen) were subjected to autoantibody monitoring across a panel of 130 antigens and the overall presentation of HSR/SR. (**A**) Autoantibody profiles and monitoring before CRT, after CRT, and after the first ICI. The antigen panel is outlined in Table S1. (**B**) A bubble chart illustrating the relationship between the fold change and difference observed post-CRT and post-1st ICI. *CRT* chemoradiotherapy, *ICI* immune checkpoint inhibitor, *MFI* mean fluorescence intensity, *WR* weak response; *SR* spark response, *HSR* hyper-spark response, *CR* recurrence-free group, *TPS* tumor proportion score, *PFS* progression-free survival.

Relationship between clinical outcomes and autoantibody response levels

To evaluate the relationship between autoantibody dynamics and clinical outcomes, autoantibody response levels were categorized into four groups; NR, WR (fold change between 1.5 and 2.0, with an MFI change of > 500), SR (fold change > 2.0, with an MFI change > 5000), and HSR (fold change > 50, with an MFI change > 10000) (Fig. 2B, S2B). The designated WR, SR, and HSR autoantibodies of each class were part of an assay panel comprising 130 autoantibodies (Figure S2).

The number of autoantibodies that exhibited WRs varied among individuals and was not significantly associated with the clinical outcomes (Figure S3). This level of immune activation suggests engagement of the cancer-immunity cycle; it does not reach the threshold required for complete immune consolidation to eliminate microtumors with ICI. Contrastingly, strong autoantibody responses, categorized as SR and HSR (SR/HSR), were observed in seven out of 20 patients (35%). Among them, five patients (71%) achieved CR, suggesting a potential association between strong autoantibody induction and favorable treatment outcomes. Antitumor immune reactions, indicated by the SR/HSR of autoantibodies, were observed only at low yet detectable levels during the pre-CRT stage. This suggested that these changes represented secondary rather than primary immune responses (Fig. 3B). To investigate the immune context of elevated autoantibody responses, we reanalyzed RNA-seq data from PBMCs using the microenvironment cell population-counter algorithm. This analysis revealed an increase in B cell abundance after the first ICI dose (Figure S4). Patients who exhibited SR/HSR showed a particularly strong increase in B cell proportion compared to those who exhibited WR and NR. The SR/HSR pattern of autoantibody responses represents a promising biomarker for predicting effective activation of the cancer immunity cycle, which is sufficient to eliminate residual microtumors during ICI therapy. Although the number of clinical samples was limited, early immune monitoring within two weeks post-first ICI may be a surrogate marker for predicting treatment outcomes. Autoantibodies exhibiting SR/HSR differ among patients, and their appearance pattern is difficult to predict. However, a panel of 130-antigens enabled the efficient capture of SR/HSR signatures and provided insight into the activation of the cancer immune cycle.

Importantly, although ICIs promote immune responses to eliminate microtumors, excessive immune activation may increase the risk of immune-related adverse events. For example, patient 5 exhibited an HSR of autoantibodies during consolidation therapy, highlighting the close relationship between the autoimmune and antitumor immune responses. This underscores the need for careful monitoring to balance therapeutic efficacy with the potential risks of immune-related complications.

Prediction of therapeutic effect by combining TPS and SR/HSR of autoantibodies

Microtumors that remain after CRT is assumed to maintain their phenotypic characteristics pre-CRT initiation. Therefore, TPS, which measures the cellular surface target antigen for ICI (PD-L1) and is determined by biopsy pre-CRT, could be a predictive marker of ICI efficacy. Patients with TPS ≥ 50% showed significantly better PFS than those with < 50%, with two-year PFS rates of 72.9% (95% CI; 46.8–100) and 20.5% (95% CI; 6.54–64.3), respectively (log-rank $p = 0.023$) (Figure S5A). A strong autoantibody response during the first two weeks of ICI consolidation therapy predicted favorable outcomes. Patients with SR/HSR responses had a significantly better two-year PFS compared to those without at 66.7% (95% CI; 37.9–100) versus 30.8% (95% CI; 13.6–69.5), respectively (log-rank $p = 0.043$) (Figure S5B). The pre-CRT TPS and post-first ICI early autoantibody responses represent two distinct and independent biomarkers for predicting the efficacy of the PACIFIC regimen. After combining these two biomarkers, patients in Group 1 who demonstrated either an SR/HSR of autoantibodies or a TPS ≥ 50% achieved CR in seven out of nine cases. Contrastingly, nine of the 11 patients in Group 2 who did not exhibit SR/HSR of autoantibodies were classified as having PD. Notably, patients L-20 and L-23, who had TPSs < 1%, were accurately classified based on the SR/HSR of autoantibodies (Fig. 4A). Group 1 had a significantly better PFS than Group 2, with two-year PFS rates of 72.9% (95% CI; 46.8–100) and 18.2% (95% CI; 5.19–63.7), respectively (log-rank $p = 0.0021$) (Fig. 4B). These findings highlight the potential of combining TPS and autoantibody SR/HSR to improve the accuracy of predicting treatment response in patients undergoing CRT or ICI therapy.

Discussion

Activation of the cancer immunity cycle is crucial for cancer immunotherapy because it enhances clinical benefits[5]. However, the efficacy of ICIs is highly variable among individuals, largely due to the influence of the tumor microenvironment and degree of antitumor immune exhaustion[25]. Transcriptomic analysis of tumor biopsies provides valuable insights into immune status by elucidating molecular networks within the tumor microenvironment[26]. However, the invasive nature of biopsy limits their repeated use in clinical practice. Currently, TPS is routinely assessed in tumor biopsies to predict the clinical benefits of first-line and postoperative ICI monotherapy in patients with NSCLC[6,27–29]. Consequently, although TPS is determined pre-CRT, its ability to accurately reflect the PD-L1 status of clinically non-detectable residual microtumors following CRT with the PACIFIC regimen remains unclear. Here, higher TPS in pre-CRT tumor biopsies was strongly correlated with the ability of patients to respond to ICI, suggesting that the PD-L1 expression phenotype of the residual primary and metastatic microtumors outside the radiation sites was preserved (Fig. 4).

The cancer-immunity cycle involves multiple steps, and TPS is not the sole determinant of immune activity[5]. Considering the inherent variability in individual responses to ICI therapy, assessing the antitumor immune response in residual microtumors is crucial for optimizing the clinical benefits of ICI as adjuvant immune consolidation therapy. Monitoring autoantibodies through minimally invasive blood tests is practical and well-suited for routine clinical practice. Multiplexed bead array assays, such as those using a Luminex analyzer, are widely employed for the clinical diagnosis of various diseases[30,31]. Thus, the MUSCAT assay panel offers significant advantages for clinical application of ICI combination therapy. As autoantibody levels increase in response to autoantigen stimulation of B cells during the secondary immune response (Fig. 3B), their concentration reflects

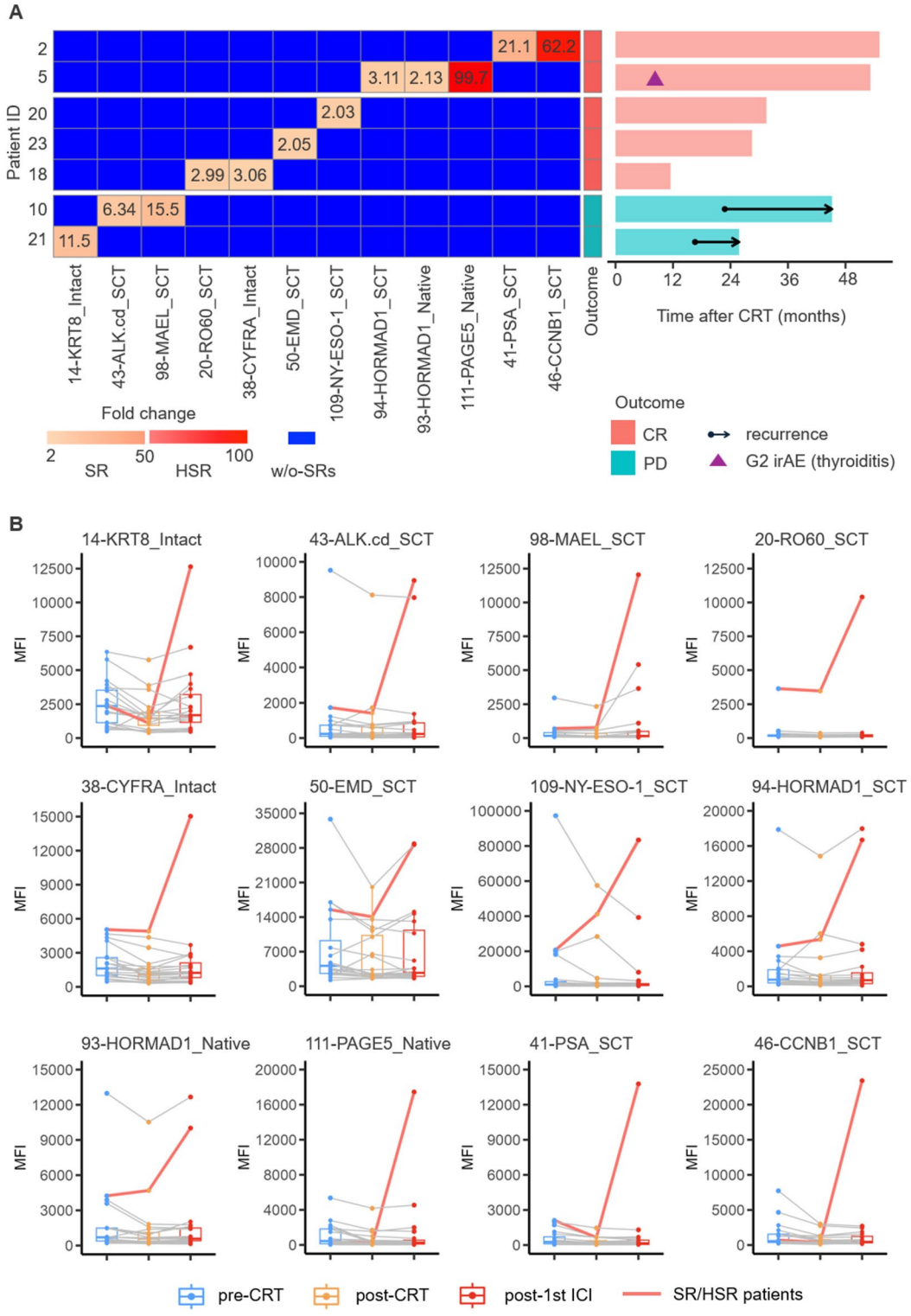

Fig. 3. Relationships between the SR/HSR and clinical outcomes. (**A**) The heatmap illustrates the fold change in the SR/HSR of autoantibodies per patient, while the bar graph displays the PFS. The values in the tiles represent the fold change. Patients with HSR of autoantibodies had prolonged PFS. (**B**) Twelve autoantibody titer changes associated with SR/HSR were detected in 20 patients. *SR* spark response, *HSR* hyper-spark response, *PFS* progression-free survival, *CRT* chemoradiotherapy, *CR* recurrence-free group, *PD* non-CR group, *ICI* immune checkpoint inhibitor, *irAE* immune-related adverse events.

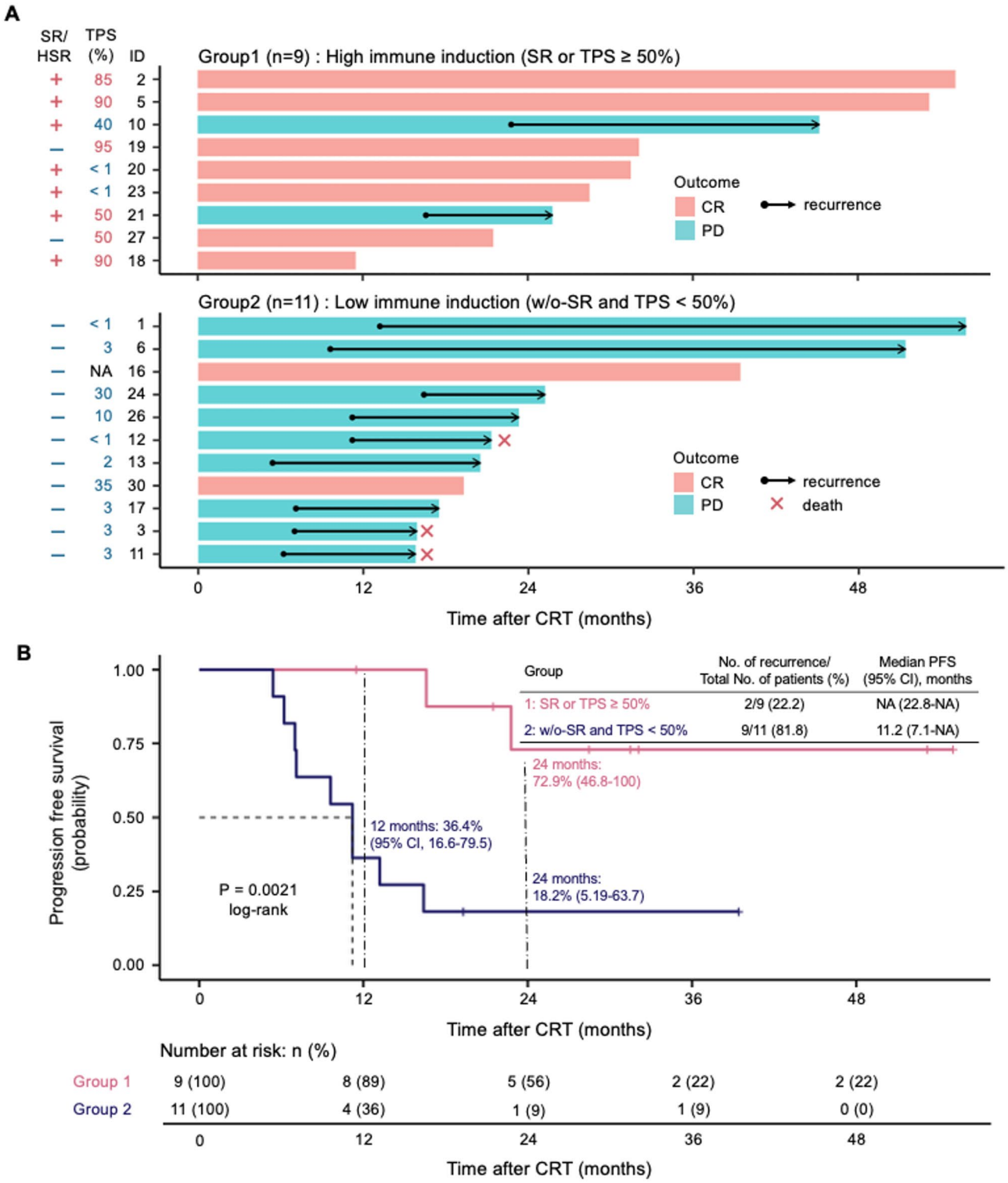

Fig. 4. Stratification of patients based on autoantibody immune response and TPS. Patients were stratified by integrating SR/HSR immune monitoring levels and ICI efficacy prediction based on the TPS. (**A**) Swimmer plots illustrating events during the observation period for Group 1 (high immune induction: SR/HSR or TPS ≥ 50%) and Group 2 (low immune induction: w/o-SRs and TPS < 50%). (**B**) Kaplan–Meier plots displaying PFS for Group 1 and Group 2 patients. The P value was derived from the log-rank test. *SR* spark response; *HSR* hyper-spark response, *TPS* tumor proportion score, *CRT* chemoradiotherapy, *PFS* progression-free survival, *CI* confidence interval.

tumor lysis and humoral immunity, indicating the status of the cancer-immunity cycle. A semi-comprehensive array was necessary to account for individual variations in autoantibody profiles (Fig. 2A, S2A).

Therefore, we focused on the autoantibody immune response during the first two weeks following the initial ICI injection. WR, defined as the detection of 0–6 of 130 autoantibodies in the panel, was observed in some patients. However, this weak response did not eliminate the microtumors (Figure S3). Contrastingly, the SR/HSR emerged as a critical indicator of successful microtumor clearance (Fig. 3). To investigate the immunological basis of SR/HSR, we assessed immune cell composition via RNA-seq analysis of PBMCs. Patients exhibiting SR/HSR showed increased B cell abundance following ICI administration (Figure S4). Because of the clinical undetectability of residual microtumors at this stage, expression analysis of antigens triggering SR/HSR in these lesions was unfeasible. However, since SR/HSR autoantibody production depends on antigen-stimulated B cell activation, we propose that these antigens are likely released from microtumors lysed by the initial ICI treatment. This hypothesis aligns with our previous findings that specific tumor antigen expression triggers strong autoantibody responses during cancer gene therapy[20].

Although our study was limited by the sample size and indirect assessment of the intratumoral immune composition, these results collectively suggest that strong autoantibody responses signify humoral immune system activation. Overall, we propose that the autoantibody spark response serves as a promising biomarker, reflecting productive engagement of the cancer-immunity cycle and predicting the eradication of clinically undetectable microtumors (Fig. 4).

Recent studies have highlighted the role of B cells, plasma cells, and tertiary lymphoid structures (TLSs) in the tumor microenvironment, linking them to improved clinical outcomes of ICI therapy in various cancers, including NSCLC, by enhancing antitumor immune activity within the tumor[5,32,33]. TLSs are estimated to disappear with tumor shrinkage owing to CRT using the PACIFIC regimen. Therefore, the autoantibody response observed in this study may have originated from the stimulation of memory B cells by specific antigens released from immunologically lysed cells, which were activated in the lymph nodes.

Here, pre-CRT TPS and strong autoantibody response during the first two weeks of ICI consolidation therapy were identified as independent biomarkers for the effectiveness of the PACIFIC regimen (Figure S5). Combining these two indices may increase the treatment outcome accuracy (Fig. 4B).

However, this study has some limitations. This retrospective study was conducted in a small cohort. Further large-scale retrospective and prospective studies are needed to validate the strong immune response observed with SR/HSR autoantibodies as predictive biomarkers for the PACIFIC regimen.

Conclusion

Patients receiving the PACIFIC regimen showed a strong autoantibody response soon after starting ICI consolidation therapy, especially those with favorable outcomes. Although TPS before CRT serves as an independent predictive biomarker, combining it with autoantibody response improves the accuracy of predicting the treatment response. Monitoring autoantibodies using the MUSCAT assay panel can reveal an antitumor immune response in clinically non-detectable residual microtumors that are enhanced by ICIs, thereby increasing the precision of treatment outcome predictions.

Data availability

The datasets generated during the current study are available from the corresponding author on reasonable request.

Received: 4 April 2025; Accepted: 15 July 2025
Published online: 28 July 2025

References

1. Antonia, S. J. et al. Durvalumab after chemoradiotherapy in stage III non-small-cell lung cancer. *N Engl. J. Med.* **377** (20), 1919–1929 (2017).
2. Antonia, S. J. et al. Overall survival with durvalumab after chemoradiotherapy in stage III NSCLC. *N Engl. J. Med.* **379** (24), 2342–2350 (2018).
3. Spigel, D. R. et al. Five-Year survival outcomes from the PACIFIC trial: durvalumab after chemoradiotherapy in stage III Non-Small-Cell lung Cancer. *J. Clin. Oncol.* **40** (12), 1301–1311 (2022).
4. Stewart, R. et al. Identification and characterization of MEDI4736, an antagonistic Anti-PD-L1 monoclonal antibody. *Cancer Immunol. Res.* **3** (9), 1052–1062 (2015).
5. Mellman, I., Chen, D. S., Powles, T. & Turley, S. J. The cancer-immunity cycle: indication, genotype, and immunotype. *Immunity* **56** (10), 2188–2205 (2023).
6. Memmott, R. M., Wolfe, A. R., Carbone, D. P. & Williams, T. M. Predictors of response, Progression-Free survival, and overall survival in patients with lung Cancer treated with immune checkpoint inhibitors. *J. Thorac. Oncol.* **16** (7), 1086–1098 (2021).
7. Doroshow, D. B. et al. PD-L1 as a biomarker of response to immune-checkpoint inhibitors. *Nat. Rev. Clin. Oncol.* **18** (6), 345–362 (2021).
8. Nemazee, D. Mechanisms of central tolerance for B cells. *Nat. Rev. Immunol.* **17** (5), 281–294 (2017).
9. Moritz, C. P. et al. Autoantigenomics: holistic characterization of autoantigen repertoires for a better Understanding of autoimmune diseases. *Autoimmun. Rev.* **19** (2), 102450 (2020).
10. de Jonge, H., Iamele, L., Maggi, M., Pessino, G. & Scotti, C. Anti-Cancer Auto-Antibodies: roles, applications and open issues. *Cancers (Basel)* **13**(4). (2021).
11. Cheever, M. A. et al. The prioritization of cancer antigens: a National cancer Institute pilot project for the acceleration of translational research. *Clin. Cancer Res.* **15** (17), 5323–5337 (2009).
12. Almeida, L. G. et al. CTdatabase: a knowledge-base of high-throughput and curated data on cancer-testis antigens. *Nucleic Acids Res.* **37** (Database issue), D816–D819 (2009).
13. Brossart, P. The role of antigen spreading in the efficacy of immunotherapies. *Clin. Cancer Res.* **26** (17), 4442–4447 (2020).

14. Ohue, Y. et al. Serum antibody against NY-ESO-1 and XAGE1 antigens potentially predicts clinical responses to Anti-Programmed cell Death-1 therapy in NSCLC. *J. Thorac. Oncol.* **14** (12), 2071–2083 (2019).
15. Sakaeda, K. et al. Automated immunoassay of serum NY-ESO-1 and XAGE1 antibodies for predicting clinical benefit with immune checkpoint inhibitor (ICI) in advanced non-small cell lung cancer. *Cancer Treat. Res. Commun.* **40**, 100830 (2024).
16. Montero-Calle, A., Garranzo-Asensio, M., Moreno-Casbas, M. T., Campuzano, S. & Barderas, R. Autoantibodies in cancer: a systematic review of their clinical role in the most prevalent cancers. *Front. Immunol.* **15**, 1455602 (2024).
17. Shome, M. et al. Serum autoantibodyome reveals that healthy individuals share common autoantibodies. *Cell. Rep.* **39** (9), 110873 (2022).
18. Ahmadi, H. et al. Unusual aggregation property of recombinantly expressed cancer-testis antigens in mammalian cells. *J. Biochem.* **170** (3), 435–443 (2021).
19. Rajagopalan, K., Mooney, S. M., Parekh, N., Getzenberg, R. H. & Kulkarni, P. A majority of the cancer/testis antigens are intrinsically disordered proteins. *J. Cell. Biochem.* **112** (11), 3256–3267 (2011).
20. Miyamoto, A. et al. Engineering cancer/testis antigens with reversible S-Cationization to evaluate antigen spreading. *Front. Oncol.* **12**, 869393 (2022).
21. Futami, J. et al. Sensitive multiplexed quantitative analysis of autoantibodies to Cancer antigens with chemically S-Cationized Full-Length and Water-Soluble denatured proteins. *Bioconjug. Chem.* **26** (10), 2076–2084 (2015).
22. Someya, M. et al. Combined chemoradiotherapy and programmed cell death-ligand 1 Blockade leads to changes in the Circulating T-cell receptor repertoire of patients with non-small-cell lung cancer. *Cancer Sci.* **113** (12), 4394–4400 (2022).
23. Date, M. et al. Hydrophobicity and molecular mass-based separation method for autoantibody discovery from mammalian total cellular proteins. *Protein Sci.* **32** (10), e4771 (2023).
24. Kimura, S., Yamamoto, W., Miyamoto, A., Imamura, K. & Futami, J. Pre-folding purification procedures for inclusion body-derived non-tagged cationic Recombinant proteins with multiple disulfide bonds for efficient refolding. *Biotechnol. Prog* e3532. (2025).
25. Baghban, R. et al. Tumor microenvironment complexity and therapeutic implications at a glance. *Cell. Commun. Signal.* **18** (1), 59 (2020).
26. Bagaev, A. et al. Conserved pan-cancer microenvironment subtypes predict response to immunotherapy. *Cancer Cell.* **39** (6), 845–(2021). – 65.e7.
27. Reck, M., Remon, J. & Hellmann, M. D. First-Line immunotherapy for non-small-cell lung cancer. *J. Clin. Oncol.* **40** (6), 586–597 (2022).
28. Hanna, N. H. et al. Therapy for stage IV non-small-cell lung cancer with driver alterations: ASCO and OH (CCO) joint guideline update. *J. Clin. Oncol.* **39** (9), 1040–1091 (2021).
29. Felip, E. et al. Overall survival with adjuvant Atezolizumab after chemotherapy in resected stage II-IIIA non-small-cell lung cancer (IMpower010): a randomised, multicentre, open-label, phase III trial. *Ann. Oncol.* **34** (10), 907–919 (2023).
30. Graham, H., Chandler, D. J. & Dunbar, S. A. The genesis and evolution of bead-based multiplexing. *Methods* **158**, 2–11 (2019).
31. Dunbar, S. A. Multiplexed suspension array immunoassays for detection of antibodies to Pneumococcal polysaccharide and conjugate vaccines. *Front. Cell. Infect. Microbiol.* **13**, 1296665 (2023).
32. Laumont, C. M., Banville, A. C., Gilardi, M., Hollern, D. P. & Nelson, B. H. Tumour-infiltrating B cells: immunological mechanisms, clinical impact and therapeutic opportunities. *Nat. Rev. Cancer.* **22** (7), 414–430 (2022).
33. Fridman, W. H. et al. Tertiary lymphoid structures and B cells: an intratumoral immunity cycle. *Immunity* **56** (10), 2254–2269 (2023).

Acknowledgements

We would like to acknowledge all the patients who participated in the study and their families.

Author contributions

Conceptualization and project supervision: M.S., M.K., J.F.; data curation and patient recruitment: M.K., T.H., M.S., T.T., T.G.; methodology: T.M., T.H., M.M., A.M., J.F.; investigation: T.M., T.H., M. D., M.M., A.M.; formal analysis: T.M., M.S., A.M.; visualization: T.M., M.M., A.M.; writing – original draft: T.M., M.K., J.F.; writing – review and editing: all authors reviewed, read, and approved the final version of the manuscript.

Funding

This work was partially supported by JST START Grant Number JPMJST1918 (JF), JSPS KAKENHI Grant Number 22H01881 (JF), 24K10913(MS), 23K14923(MK), 23K07161(TT), 24K23389(AM) JST SPRING, Grant Number JPMJSP2126 (TM), Grant-in-Aid for JSPS Fellows 24KJ1711 (MD), grant from Japanese Society of Hematology (MM), Science and Technology Promotion grants (2019–2024) in the Okayama Prefecture, Japan (JF).

Declarations

Competing interests

The authors declare no competing interests.

Consent for publication

J.F. and Medinet Co., Ltd. hold patents for the MUSCAT assay method.

Additional information

Supplementary Information The online version contains supplementary material available at https://doi.org/10.1038/s41598-025-12069-5.

Correspondence and requests for materials should be addressed to J.F.